IEEE Access
Multidisciplinary | Rapid Review | Open Access Journal

Received July 14, 2020, accepted July 24, 2020, date of publication July 28, 2020, date of current version August 7, 2020.

Digital Object Identifier 10.1109/ACCESS.2020.3012431

Use of Two Open-Terminated Coaxial Transmission-Lines Technique to Extract the Material Relative Intrinsic Parameters

FRANCK MOUKANDA MBANGO[1], JOSUÉ ERIC DELFORT M'PEMBA[1], FABIEN NDAGIJIMANA[2], AND BERNARD M'PASSI-MABIALA[3,4]

[1]Electrical and Electronics Department, Marien Ngouabi University, Brazzaville BP: 69, Republic of Congo
[2]Department of Electrical Engineering, Université Grenoble Alpes, CNRS, Grenoble INP, G2ELab, 38400 Saint-Martin d'Hères, France
[3]Groupe de Simulations Numériques en Magnétisme et Catalyse, Marien Ngouabi University, Brazzaville BP: 69, Republic of Congo
[4]Unité de Recherche en Sciences Exactes et Naturelles (IRSEN), Brazzaville BP: 69, Republic of Congo

Corresponding author: Franck Moukanda Mbango (franck.moukandambango@umng.cg)

ABSTRACT We have presented an open-terminated transmission-line technique, based on the use of two substantially identical circular coaxial structures with different lengths, to extract the material relative permittivity ε_r. All data acquisitions obtained from experimental measurements have been done at the entry of the connector-input source interface. The technique is well-utilized despite the test cell discontinuity, and it met the goal of extracting the relative intrinsic parameters with good accuracy. The technique improvement found its advantage in the scan of a large frequency range by introducing a new concept based upon the sum of the lengths of identical fixtures and the backward wave propagation. High order-modes propagation that restricts the frequency range in the transmission configuration is not a limit in this new technique. Otherwise, the measurement methodology, grounded in the principle of the automatic correction coefficient determination, is done to achieve the aim. Easily filling up the test cell with the sample to characterize, we validated the new broadband technique in [1.5 – 15] GHz by using insulators like Aquarium sand, wheat semolina, and raffia (vinifera and laurentiis varieties). From the use of the same fixture, result comparisons have been done with those from the two-line technique.

INDEX TERMS Material characterization, Maxwell equation, measurement technique, open-terminated line, propagation constant, transmission-line.

I. INTRODUCTION

New technology developments require researchers to develop new material method characterizations. Constraints associated with material dimensions, technique accuracy, and scanned frequencies are nowadays a significant challenge that requires a deep and good study on techniques to be used. Two main methods with several techniques enhance the literature: distributed and lumped elements [1]. The distributed element technique, using iterative method [2] and/or transmission-line propagation constant [3]–[5], is a well-known technique. As methods can be destructive or not [6], researchers are in the habit of using the transmission structure in short-circuit [7] and/or open-circuit [8] configurations along with reflection/transmission [9] in order to get to the material intrinsic parameters.

From the open-ended probe configuration [10], [11], the sample under test (SUT) is inserted in a test cell that has an open-terminated configuration. The open-terminated line technique (OTLT), becomes an alternative [1] and [8], but most of the time, the iterative method is applied as equation (1) says.

$$\left(\frac{Z_v}{Z_{SUT}}\right)_{in} = \sqrt{\frac{\varepsilon_r}{\mu_r}}\frac{\tan\left(\beta_v l\sqrt{\varepsilon_r\mu_r}\right)}{\tan\left(\beta_v l\right)} \tag{1}$$

where β_v is the phase constant in vacuum test cell configuration, l the cell length, and Z_v and Z_{SUT} are characteristic impedance measured from the input of the test cell. On the other hand, discontinuities, together with the

The associate editor coordinating the review of this manuscript and approving it for publication was Andrei Muller.

fixture's dimensions, generate high order modes, limiting the study frequency range [12], [13]. Usually, the material under test is placed at the end of the probe adopted as a characterization technique. That configuration is quite often an open-circuit. However, the technique implemented here uses a coaxial line structure in which the sample under test is inserted while the fixture is opened at its end. This kind of configuration can behave like an antenna according to the scanned frequency and the fixture dimensions.

In this article, the developed and presented technique is focused on the use of two coaxial transmission lines with open-termination. The use of two different lengths of the line (cell) avoids applying the iterative principles. Both test cells have the same geometric dimensions, except their lengths. For this reason, we identify the technique as the two open circuit position method. The open-circuit movable position is a reflection technique, using the sum of lengths via the phase constant in order to determine the material relative permittivity. The technique does not involve the extraction of the loss tangent but solves the discontinuity problem, depending on the frequency range limitation. That offers the possibility of scanning a large frequency range. The two transmission-line technique is one of the best-known and most popularly used techniques [3], [4]. It is based on the use of the wave cascading matrix (WCM), well-developed in [14], [15] with the use of the difference of the length via the propagation constant. That technique has inspired our approach to developing the new technique.

II. BASIS OF EXTRACTION TECHNIQUES

Electromagnetic material characterization is a fundamental activity for all industrial domains (e.g., microelectronics, telecommunications, civil engineering, biotechnology, and electronics). Based on the use of Maxwell equations, most of the techniques use the propagation constant parameter to identify wave behaviors in propagation environments. As a matter of fact, solving the Maxwell-Ampere equation, given as follows,

$$\overrightarrow{rot}\vec{B} = \mu(\sigma + j\omega\varepsilon)\vec{E} \tag{2}$$

associated with the Maxwell-Faraday equation given in (3) as

$$\overrightarrow{rot}\vec{E} = -j\omega\vec{B} \tag{3}$$

The propagation constant parameter is obtained and given as,

$$\gamma = \sqrt{j\omega\mu(\sigma + j\omega\varepsilon)} \tag{4}$$

where,

$$\mu = \mu_0\mu^*_{eff}$$

and

$$\varepsilon = \varepsilon_0\varepsilon^*_{eff}$$

are material intrinsic parameters (respectively permeability and permittivity). The permeability and permittivity of the vacuum are ε_0 and μ_0. The need to know the material electric and/or magnetic parameters is growing with industrial applications. Therefore, several techniques have been developed according to the method to be used [16], fitting the material shape and physical state together with the frequency range to be covered [1], [5], and [17]. If the test cell has a homogeneous structure, then the relative complex permittivity and/or permeability are the effective parameters as given in equation (5).

$$\varepsilon^*_{eff} = \varepsilon^*_r \tag{5a}$$
$$\mu^*_{eff} = \mu^*_r \tag{5b}$$

Those elements are complex and written as given [18] below,

$$\varepsilon^*_r = \varepsilon'_r - j\varepsilon''_r \tag{6a}$$
$$\mu^*_r = \mu'_r - j\mu''_r \tag{6b}$$

If the material is assumed to be insulator or magnetic, then the sample under test (SUT) parameters μ^*_r and ε^*_r are obtained from equation (4) by,

$$\varepsilon'_r\mu'_r = \left(\frac{\beta_{SUT}}{\beta_v}\right)^2 \tag{7}$$

Although related to the phase constant which has to be linearized, the order propagation modes generated by the fixture dimensions and imperfections at the contact interface between connectors and the ideal line (called discontinuity) nearly stop in the frequency range with which we are concerned. The transmission-line technique is one of the popular trade-off techniques [5]. Sometimes, open or short-circuit line configurations are used but are limited by the use and accuracy of iterative processes [1]. For this reason, we are interested in the developed open-ended configuration transmission-line technique, which uses two different lengths of the same test cell to overcome these limitations.

III. TECHNIQUE IMPLEMENTATION

Equation (4) says that propagation constant is complex and from wave vector through Maxwell equation development, we have:

$$\gamma = \alpha + j\beta \tag{8}$$

As Fig 1, shows, the de-embedding of such structure is given by:

$$\Gamma = \left(S^g_{11}\right)_{CO}\exp\left(2\gamma_0 l_0\right) \tag{9}$$

where $\left(S^g_{11}\right)_{CO}$ is the reflection coefficient, measured at the input reference (interface input source and connector) plan and Γ the equivalent reflection coefficient after having de-embedded or changed the reference plan (interface connector and ideal test cell).

From studies using Agilent Design System (ADS), we noticed that discontinuity impedance $Z_d \approx \infty$, which means at connector – test cell interface contact, the discontinuity impedance is almost an open circuit. In that case,

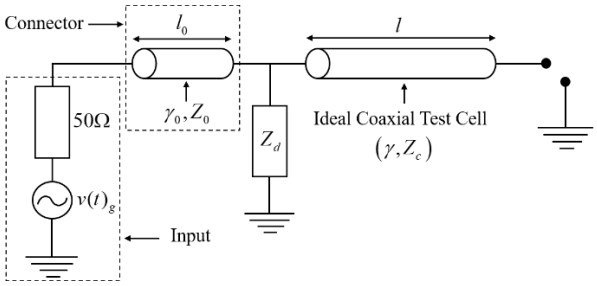

FIGURE 1. An open-terminated transmission-line configuration simplified representation.

the phase constant βl is nearly those coming from the de-embedding.

$$(\beta l)_{\text{real}} \cong (\beta l)_{\text{meas}} \tag{10}$$

where

$$(\gamma l)_{\text{meas}} = -\frac{1}{2}\ln\left(\frac{\Gamma}{|\Gamma|}\right) \tag{11}$$

Fig 1. is the simplification of the manufactured fixture as shown below:

As the discontinuity impact is insignificant, Fig 1. has been reduced as shown in Fig 2. below,

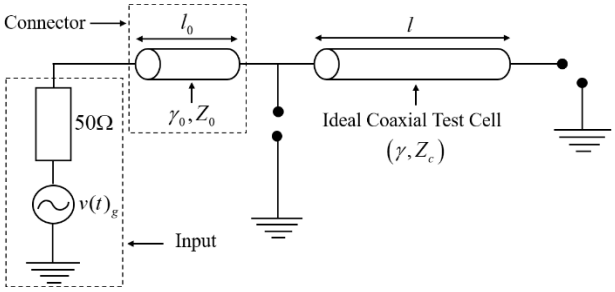

FIGURE 2. Final open-terminated transmission-line configuration.

Using two different test cell lengths where $\beta_1 = \beta_2 = \beta$ applying equation (7) allows establishing that:

$$\varepsilon'_r\mu'_r = \left\{\frac{(\beta l_T)_{SUT}}{(\beta l_T)_v}\right\}^2 \tag{12a}$$

where

$$\beta l_T = \beta\,(l_2 + l_1) = \beta\,(2l_1 + \Delta l) \tag{12b}$$

and,

$$\Delta l = l_2 - l_1$$

It appears that the technique is the sum of lengths in each configuration. In that case, rewriting equation (12a) gives,

$$\varepsilon'_r\mu'_r = \left\{\frac{(\beta\,(2l_1 + \Delta l))_{SUT}}{(\beta\,(2l_1 + \Delta l))_v}\right\}^2 = \left\{\frac{(\Delta T)_{SUT}}{(\Delta T)_v}\right\}^2 \tag{13}$$

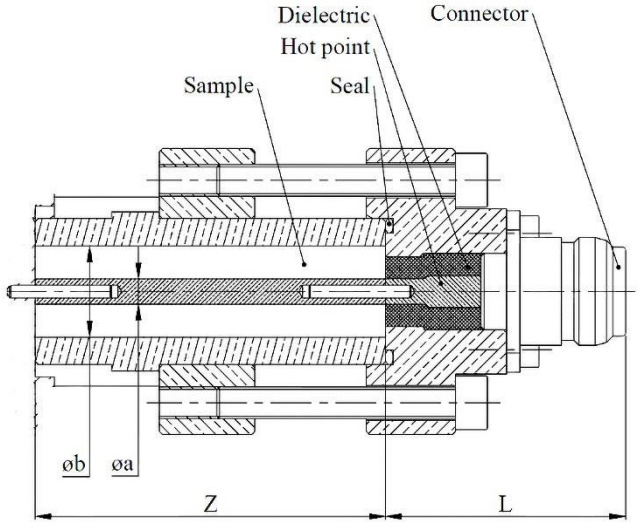

FIGURE 3. Test cell model in open-terminated configuration.

If we label by Z_{in}^{SC} and Z_{in}^{OC}, respectively, the input connector impedances in short-circuit and open-circuit configurations, the connector propagation constant is calculated as it's given below:

$$\gamma_0 l_0 = \tanh^{-1}\left[\left(\frac{Z_{in}^{SC}}{Z_{in}^{OC}}\right)^{\frac{1}{2}}\right] \tag{14a}$$

Using reflection coefficient S_{11}^C at that reference plan, the input impedance requires being determined as,

$$Z_{in} = Z_n\frac{1 + S_{11}^x}{1 - S_{11}^x} \tag{14b}$$

where S_{11}^x is the connector reflection coefficient, measured in open-circuit or short-circuit termination. Most of the time, electronic RF equipment admits an input impedance $Z_n = 50\ \Omega$. In addition, when the test cell is filled with a sample under test or vacuum, from equations (8), (9) and (11), the computed phase constants become,

$$(\beta l)_{SUT} = \text{Im}\left[-\frac{1}{2}\ln\left(\frac{(S_{11}^g)_{SUT}\,e^{2\gamma_0 l_0}}{|(S_{11}^g)_{SUT}\,e^{2\gamma_0 l_0}|}\right)\right] \tag{15a}$$

$$(\beta l)_v = \text{Im}\left[-\frac{1}{2}\ln\left(\frac{(S_{11}^g)_v\,e^{2\gamma_0 l_0}}{|(S_{11}^g)_v\,e^{2\gamma_0 l_0}|}\right)\right] \tag{15b}$$

The use of equation (15) is purposely called "old concept" because it employs the forward wave propagation during the de-embedding procedure. On the other hand, the electric angular position $\beta l = \theta$ is linearized and symbolized by φ before being applied in equation (12b). The global linearized phase constant in a certain configuration is $\Delta T = \varphi_1 + \varphi_2$: $(\Delta T)_v$ for fixture filled with vacuum and $(\Delta T)_{SUT}$ when filled with *SUT*. Due to the fixture radiation behavior, the open-circuit technique approach is valid only from

5 GHz around, and at the same time, we have improved the technique.

IV. IMPROVING TECHNIQUE

To solve the frequency range limitation, we have developed a new concept, based on the wavenumber k_0 direction in the probe (connector). It It applies electromagnetic theory to equation (8) and gives:

$$jk_0 = \alpha_0 + j\beta_0 = \gamma_0 \Rightarrow j\gamma_0 = -(\beta_0 - j\alpha_0) = -k_0$$

Due to the wave propagation direction, we have inserted the use of the backward wave principle and, equation (9) becomes as given below,

$$(\Gamma)_N = \left(S_{11}^g\right)_{CO} \exp\left(2j\gamma_0 l_0\right) \tag{16}$$

where "subscript letter "N" means new concept. The new concept, rooted in the insertion of the multiplicative imaginary element "j" gives the opportunity to employ the backward wave principle. That parameter "j" straightens wiggly lines or curves, brought on by multipath reflections into the guide through data acquisitions. The problem has been found out in both configurations as follows: with and without MUT. As the study concerns the open-ended structure, we can simply write $S_{11}^g = \left(S_{11}^g\right)_{CO}$, and for each configuration (presence of SUT or vacuum), we write respectively $\left(S_{11}^g\right)_{SUT}$ or $\left(S_{11}^g\right)_v$. In that case, the new computed phase constants are:

$$((\beta l)_{SUT})_N = \mathrm{Im}\left[-\frac{1}{2}\ln\left(\frac{\left(S_{11}^g\right)_{SUT} e^{2j\gamma_0 l_0}}{\left|\left(S_{11}^g\right)_{SUT} e^{2j\gamma_0 l_0}\right|}\right)\right] \tag{17a}$$

$$((\beta l)_v)_N = \mathrm{Im}\left[-\frac{1}{2}\ln\left(\frac{\left(S_{11}^g\right)_v e^{2j\gamma_0 l_0}}{\left|\left(S_{11}^g\right)_v e^{2j\gamma_0 l_0}\right|}\right)\right] \tag{17b}$$

As we have previously written equation (15), we noted by $(\Delta T)_N = (\varphi_1)_N + (\varphi_2)_N$ that the global linearized phase constant got from the improvement concept, where $(\varphi_1)_N$ and $(\varphi_2)_N$ represent the computed phase constant in each configuration for test cell having l_1 and l_2 as lengths. Thereby, two elements B and G are incorporated to overcome the "j" insertion effects as:

$$G = \frac{\sum((\Delta T)_{SUT})_N}{\sum(\Delta T)_{SUT}} = \frac{\sum\left[\left((\varphi_1)_{SUT}\right)_N + \left((\varphi_2)_{SUT}\right)_N\right]}{\sum\left[(\varphi_1)_{SUT} + (\varphi_2)_{SUT}\right]} \tag{17c}$$

$$B = \frac{\sum((\Delta T)_v)_N}{\sum(\Delta T)_v} = \frac{\sum\left[\left((\varphi_1)_v\right)_N + \left((\varphi_2)_v\right)_N\right]}{\sum\left[(\varphi_1)_v + (\varphi_2)_v\right]} \tag{17d}$$

In that case, equation (13) is re-written as follow,

$$\varepsilon_r'\mu_r' = \left(\frac{B}{G}\right)^2 \left\{\frac{\left((\varphi_1)_{SUT}\right)_N + \left((\varphi_2)_{SUT}\right)_N}{\left((\varphi_1)_v\right)_N + \left((\varphi_2)_v\right)_N}\right\}^2 \tag{18}$$

The automatic correction coefficient, given by $H = \left(\frac{B}{G}\right)^2$ depends on the material under test and the frequency range to be covered. This new development technique step helped to cover frequency lower than 3 GHz when using a coaxial test cell with $b = 14.36$ mm (coaxial inner diameter of the outer conductor) and $a = 4$ mm (coaxial outer diameter of the inner conductor). In this new technique, errors are high when scanning frequencies [1.5 - 4] GHz. The accuracy can reach up to 7%, but it decreases to around 3% when frequencies increase to 4 GHz and higher. If we assume that the SUT is not magnetic ($\mu_r' \approx 1$), applying equation (18) leads to extraction of the material relative permittivity, otherwise, the relative permeability is extracted by supposing the material is not electric ($\varepsilon_r = 1$). Above all, the use of equation (18) requires four linearized phase constants or electric angular θ along with two measurements for each test cell length.

V. EXPERIMENTAL TECHNIQUE VALIDATION

After some huge and deep studies through electric and electromagnetic simulations, we have validated the broadband technique by using a brass circular coaxial test cell. With $l_1 \approx 80$ mm and $l_2 \approx 100$ mm, and due to the cell diameter dimensions, the higher-order modes are supposed to propagate from 10.4 GHz when the test cell is vacuum-filled in theory [1] and working in reflection/transmission. That frequency has typically been the limitation of two transmission-line techniques. However, the new open-end transmission-line technique overcomes that frequency limitation, as shown in the results below. Due to the non-availability (in our laboratory) of conventional test samples such as PTFE, PFA, PEEK, and so forth, we experimentally validated the technique implementation and process by using semolina, laurentiis, vinifera, and aquarium sand, all of which are insulator materials.

To check the credibility of our results, we have applied the two transmission-lines technique (TTLT) to the same materials in the same test cells [3]. Those results are sketched below, but because of order mode limitations [3]–[5], the comparison is made up to 10.5 GHz while those coming from the newly presented technique reached 15 GHz.

We first presented the electric length in both configurations by plotting the aquarium sand results as MUT.

and

Using the device across the insertion of the backward wave principle has provided an opportunity to change the shape of curves, as well as heightening data values. It justified having introduced factor H to get to the main goal.

These results indicate that using equation (18) is better than using (13). Curves coming from the two transmission-line technique (TTLT) and the one using equation (18) are in close proximity, while the sketched curve got by using equation (13) is not closely related in this part of the frequency range.

This comparison technique results confirm that the new technique is suitable for extracting the material relative permittivity when using equation (18).

We have observed the same behavior when applying the implementation procedure technique to the raffia palm tree,

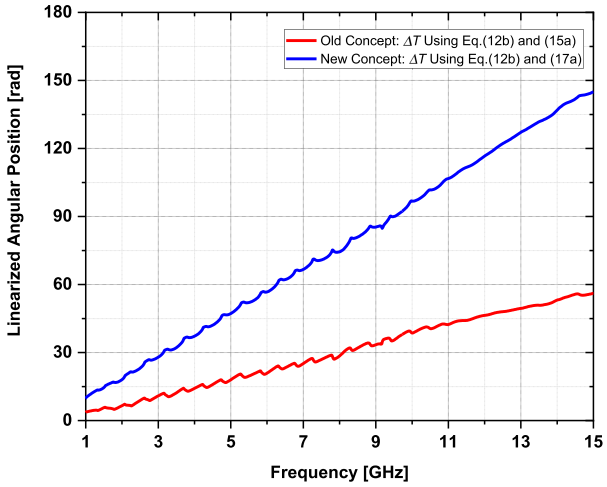

(a)

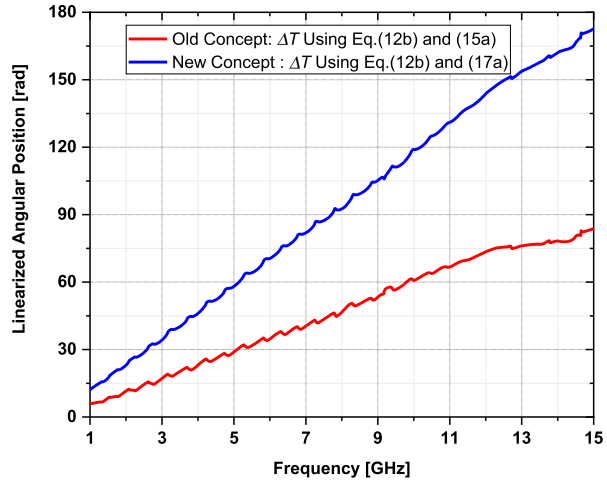

(b)

FIGURE 4. a. Linearized angular position curves of the vacuum according to the applied concept. b. Linearized angular position curves of the aquarium sand according to the applied concept.

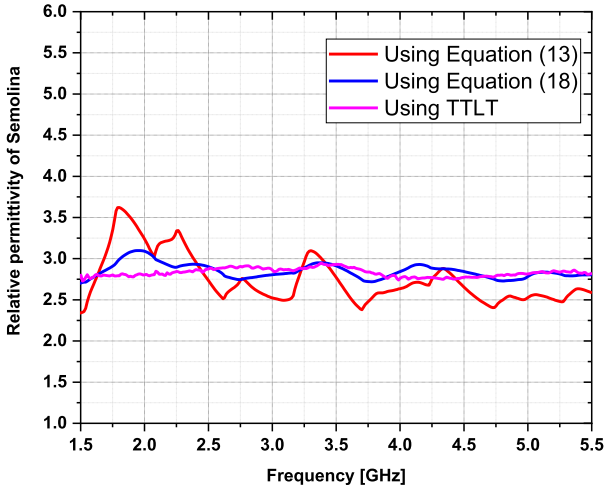

FIGURE 5. Comparison of techniques and development for semolina relative permittivity.

vinifera. Despite the fact that using equation (13) doesn't eliminate properly waves generated by the waveguide

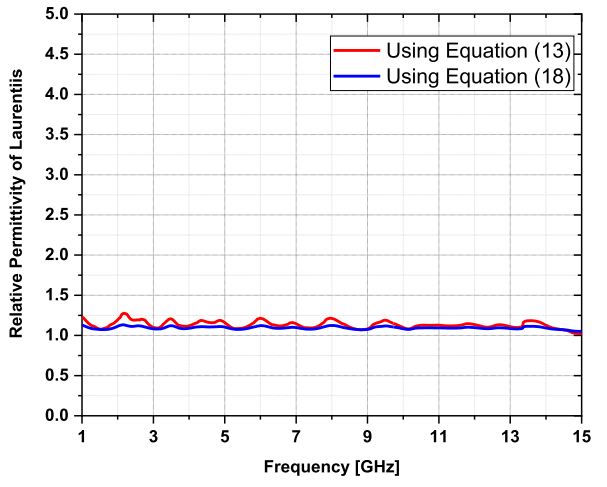

(a)

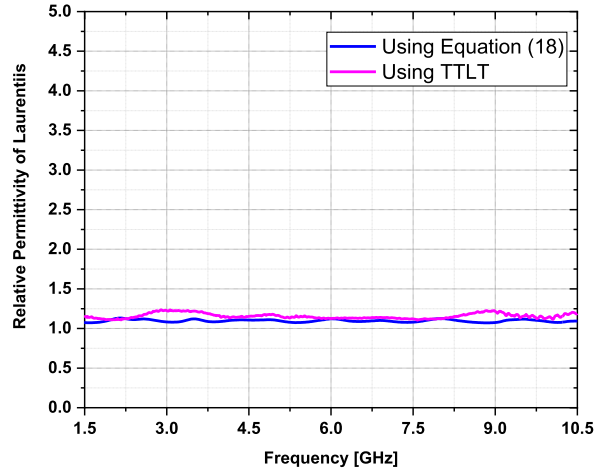

(b)

FIGURE 6. a. Comparison of two equation applications to extract Laurentiis relative permittivity. b. Comparison of technique's applications to extract Laurentiis relative permittivity.

because of multi resonances, we noticed that beyond a certain frequency (approximately 9 GHz here), both results (Fig 6a, Fig 7a, and Fig 8a) are very similar. So we have compared those results with those obtained from TTLT [3] as shown in Figs. 6b, 7b, and 8b.

All results show that it is suitable to use the transmission-line in an open configuration when the test fixtures have variable lengths, but with the same geometric shape. Applying equation (18) is suitable as the table indicates.

Considering the frequency range [2 - 12] GHz from Fig 9 and using a single or/and transmission line as well as two transmission line techniques with and without correction, terminated by an open-circuit configuration, it is clearly observed that the developed method using equation (18) is more suitable in comparison to those transmission line techniques as illustrated in Fig 10.

Below is the comparison of values obtained at 2.5 GHz, which teaches the uselessness of applying the one transmission-line technique when terminated by an open-circuit

TABLE 1. Comparison of relative permittivity values from two main techniques.

		Material relative permittivity at 2.5 GHz			
		Semolina	Laurentiis	Aquarium sand	Vinifera
OTLT	ε_{r_1} for $l_1 \approx 80$ mm	3.197	1.372	3.125	1.274
	ε_{r_2} for $l_2 \approx 100$mm	2.451	1.081	2.358	1.054
	Average of ε_{r_1} and ε_{r_2}	2.824	1.227	2.741	1.164
	Use of Eq. (13)	2.731	1.192	2.648	1.138
	Use of Eq. (18)	2.901	1.137	2.68	1.089
TTLT	Use of Δl through WCM principle	2.875	1.159	2.693	1.079

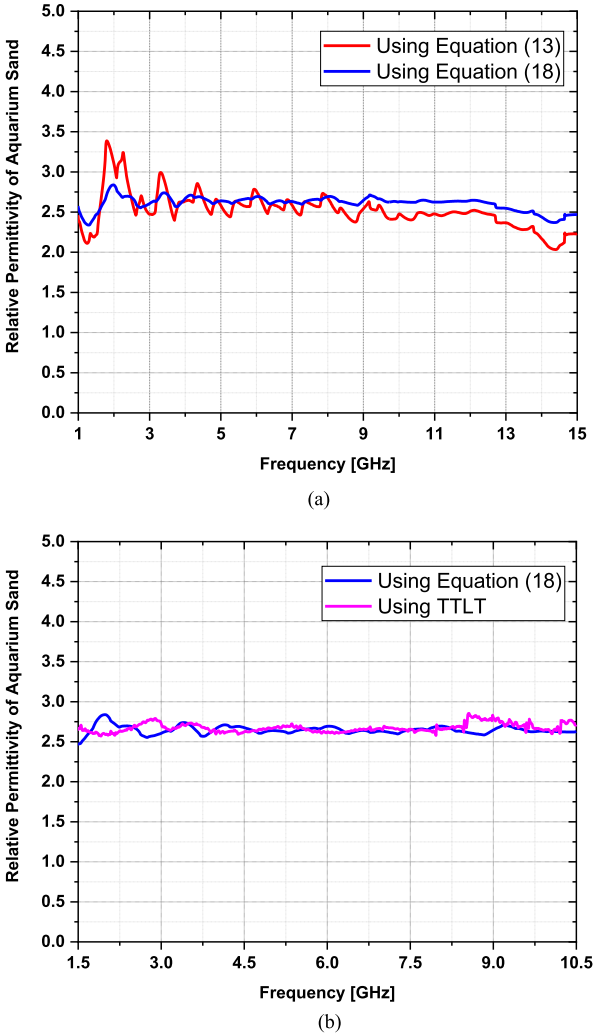

FIGURE 7. a. Comparison of two equation applications to extract Aquarium sand relative permittivity. b. Comparison of technique's applications to extract Aquarium sand relative permittivity.

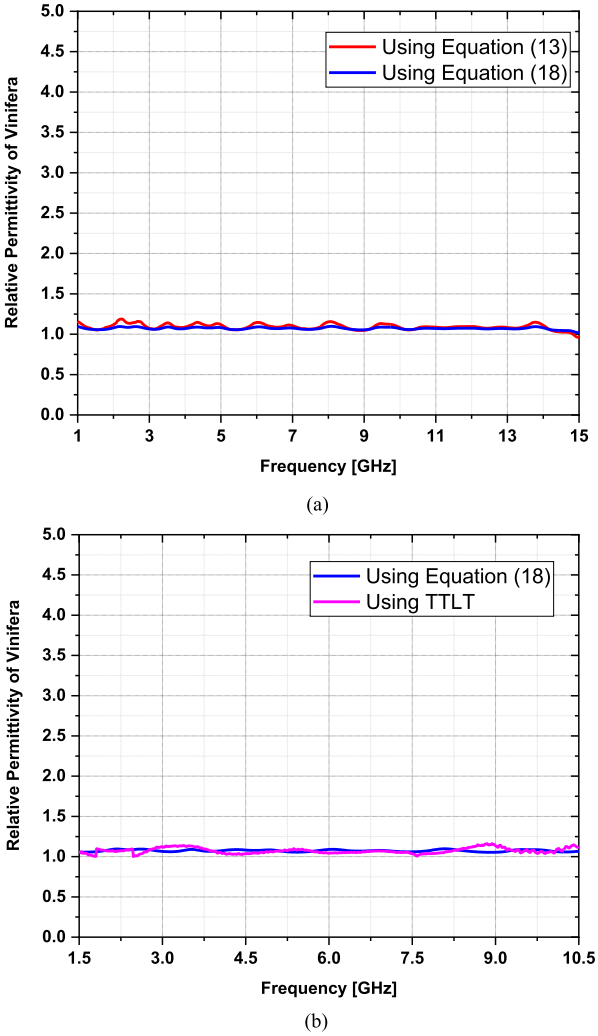

FIGURE 8. a. Comparison of two equation applications to extract Vinifera relative permittivity. b. Comparison of technique's applications to extract Vinifera relative permittivity.

configuration. In order to compare the final results, let us consider the two transmission-line technique (TTLT) and the open-terminated line technique (OTLT).

The two transmission-line techniques yielded results with incertitude or a relative error of 3-7%, depending on the frequency used [15]. By the way, the open-terminated transmission-line technique has shown that limitation is bound up with the high-order mode propagations. Due to that situation, the quasi transverse electro-magnetic (Quasi-TEM) mode is limited in scanned frequency computed through equation (19).

As equation (18) says, H-coefficient is proportional to the corrected relative permittivity. On the other hand, different values of B are due to the scanned frequency range.

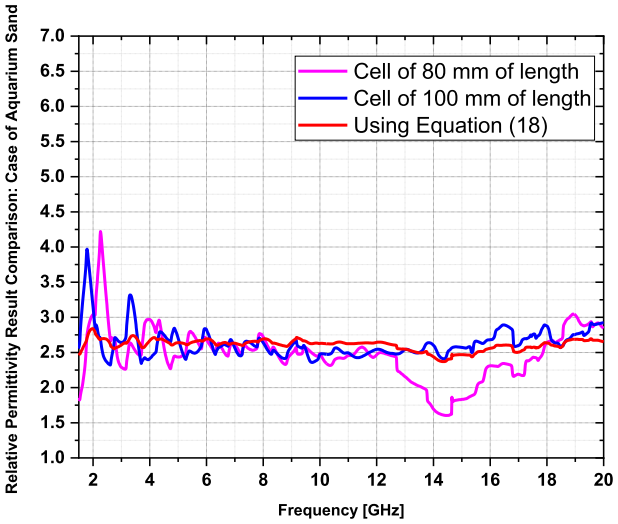

FIGURE 9. Different open-terminated transmission-line technique principles comparison.

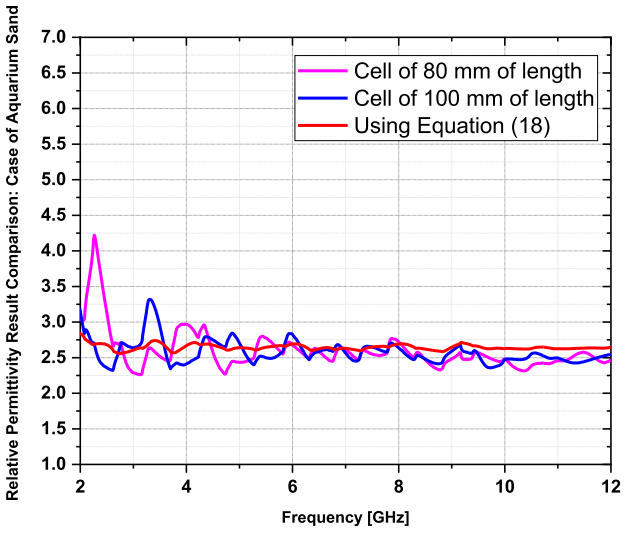

FIGURE 10. Zoom of scanned frequency of different open-terminated transmission-line technique principles comparison.

Therefore, semolina is up to 5.5 GHz, vinifera up to 15 GHz, and aquarium sand extends to 20 GHz and 18 GHz for laurentiis. This explains the proximity of vinifera, laurentiis, and aquarium sand values. In other words, B-coefficient does not change as long as the studied frequency band is the same. But G-coefficient changes with the MUT. The coefficient determinations through equation (17c) and (17d) have given the opportunity not to use specific mathematic algorithms through iterative principles like Newton-Raphson [19]. From the dimensions mentioned above, the maximum frequency TEM-mode expected in theory is 10.4 GHz [1].

$$f_{\max^{TEM}}(GHz) \cong \frac{191}{(b+a)\sqrt{\varepsilon_r \mu_r}} \tag{19}$$

where "a" is the outer diameter of the inner conductor and "b" the inner diameter of the outer conductor. Both values are given in millimeters (mm).

TABLE 2. Comparisons of coefficient values according to the material under test.

Material's name	Coefficient according to equations (17c) and (17d)		
	Coefficient B (vacuum)	Coefficient G (SUT)	Coefficient H
Semolina	2.85	2.092	1.855
Aquarium sand	2.711	2.054	1.741
Laurentiis	2.693	2.599	1.073
Vinifera	2.68	2.594	1.067

VI. CONCLUSION

In this article, we have developed and applied a technique based on the use of the sum of two open-end coaxial transmission-lines to extract the material relative permittivity or permeability. Simple to implement, the technique is broadband and covers easily frequency range [1.5-15] GHz. We have shown the importance of using equation (18) which is related to equation (9) through its propagation constants that have helped to determine automatically the H-coefficient. Aside from the purely technical aspect that structure limitations are caused by the antenna behavior, the test fixture radiates when it reaches a certain level of microwave frequencies, resulting in a loss of accuracy. All materials that have been used to validate this new extraction procedure confirmed the test cell behavior from 14 GHz. Thus, it appears that the limitation is caused exclusively by structural mechanics. The newly developed technique is not connected to the iterative principle. We have compared all extracted results derived from two transmission-line techniques, using the same frame. The discrepancy between them is very small, especially from 4.5 GHz. The technique error evaluation leads toward 5% and less. Results from the use of two lines in transmission and open-end configurations have taught that the order-modes that have typically hindered the two transmission-line technique procedure above a certain frequency are not a limitation in this new technique. Like all techniques built upon the reflection principle, this technique cannot extract the material loss tangent. This is well-adapted to industry applications, as the used test cell eases its padding with the material under test.

ACKNOWLEDGMENT

The authors would like to thank R. Batota and F. Kuhlman for helpful suggestions and the anonymous reviewers for their attentive revision and thorough assessment.

REFERENCES

[1] F. Moukanda Mbango, *Contribution A La Caractérisation des Matériaux Utilisés en Microélectronique RadioFréquence*. Saint-Martin-d'Hères, France: Joseph Fourier Univ., 2008.
[2] N. Jebbor and S. Bri, "A microwave method for complex permittivity extraction of thin materials," *J. Microw., Optoelectron. Electromagn. Appl.*, vol. 11, no. 2, pp. 285–295, Dec. 2012, doi: 10.1590/S2179-10742012000200006.
[3] F. Moukanda Mbango, A. Al Takach, and F. Ndagijimana, "Complex relative permittivity extraction technique of biotechnology materials in microwaves domain," *Int. J. Electron., Commun. Instrum. Eng. Res. Develop.*, vol. 9, no. 1, pp. 33–42, Jun. 2019, doi: 10.24247/ijecierd-jun20195.

[4] J. Baker-Jarvis, E. J. Vanzura, and W. A. Kissick, "Improved technique for determining complex permittivity with the transmission/reflection method," *IEEE Trans. Microw. Theory Techn.*, vol. 38, no. 8, pp. 1096–1103, Aug. 1990, doi: 10.1109/22.57336.
[5] M. D. Janezic and J. A. Jargon, "Complex permittivity determination from propagation constant measurements," *IEEE Microw. Guided Wave Lett.*, vol. 9, no. 2, pp. 76–78, Feb. 1999, doi: 10.1109/75.755052.
[6] S. L. S. Severo, Á. A. A. D. Salles, B. Nervis, and B. K. Zanini, "Non-resonant permittivity measurement methods," *J. Microw., Optoelectron. Electromagn. Appl.*, vol. 16, no. 1, pp. 297–311, Mar. 2017, doi: 10.1590/2179-10742017v16i1890.
[7] A. Lewandowski, A. Szypłowska, M. Kafarski, A. Wilczek, P. Barmuta, and W. Skierucha, "0.05-3 GHz VNA characterization of soil dielectric properties based on the multiline TRL calibration," *Meas. Sci. Technol.*, vol. 28, no. 2, pp. 1–7, Feb. 2017, doi: 10.1088/1361-6501/28/2/024007.
[8] J. Hinojosa, "Dielectric permittivity measuring technique of film-shaped materials at low microwave frequencies from open-end coplanar waveguide," *Prog. Electromagn. Res. C*, vol. 5, pp. 57–70, 2008.
[9] F. Moukanda Mbango and F. Ndagijimana, "Electric parameter extractions using a broadband technique from coaxial line discontinuities," *Int. J. Sci. Res. Manage.*, vol. 7, no. 5, pp. 48–53, May 2019, doi: 10.18535/ijsrm/v7i5.ec01.
[10] T. P. Marsland and S. Evans, "Dielectric measurements with an open-ended coaxial probe," *Proc. Inst. Elect. Eng., Microw., Antennas, Propag.*, vol. 134, no. 4, pp. 341–349, Aug. 1987, doi: 10.1049/ip-h-2.1987.0068.
[11] N. I. Sheen and I. M. Woodhead, "An open-ended coaxial probe for broadband permittivity measurement of agricultural products," *J. Agricult. Eng. Res.*, vol. 74, no. 2, pp. 193–202, Oct. 1999, doi: 10.1006/jaer.1999.0444.
[12] K. Zhou, W. Du, Y. Li, J. Kang, L. Zhang, Y. Hu, H. Tan, Z. Wang, S. Gao, D. Wu, and C. Tang, "Suppression of higher-order modes in a large-optical-cavity waveguide structure for high-power high-efficiency 976-nm diode lasers," *Superlattices Microstruct.*, vol. 129, pp. 40–46, May 2019, doi: 10.1016/j.spmi.2019.03.009.
[13] N. L. Aleksandrov, A. V. Chirkov, G. G. Denisov, D. V. Vinogradov, W. Kasparek, J. Pretterebner, and D. Wagner, "Selective excitation of high-order modes in circular waveguides," *Int. J. Infr. Millim. Waves*, vol. 13, no. 9, pp. 1369–1385, Sep. 1992, doi: 10.1007/BF01009994.
[14] M. Moukanda, F. Ndagijimana, J. Chilo, and P. Saguet, "Complex permittivity using two transmission line S-parameter measurements," *Afr. Phys. Rev.*, vol. 2, no. 30, pp. 1–3, 2008.
[15] A. A. Takach, F. M. Moukanda, F. Ndagijimana, M. Al-Husseini, and J. Jomaah, "Two-line technique for dielectric material characterization with application in 3D-printing filament electrical parameters extraction," *Prog. Electromagn. Res. M*, vol. 85, pp. 195–207, 2019, doi: 10.2528/pierm19071702.
[16] R. Zajíček, J. Vrba, and K. Novotný, "Evaluation of a reflection method on an open-ended coaxial line and its use in dielectric measurements," *Acta Polytech.*, vol. 46, no. 5, pp. 50–54, 2006, doi: 10.14311/882.
[17] D. M. Pozar, *Microwave Engineering*, 3rd ed. Hoboken, NJ, USA: Wiley, 2005.
[18] D. Hachi, N. Benhadda, B. Helifa, I. K. Lefkaier, and B. Abdelhadi, "Composite material characterization using eddy current by 3D FEM associated with iterative technique," *Adv. Electromagn.*, vol. 8, no. 1, pp. 8–15, Mar. 2019, doi: 10.7716/aem.v8i1.953.
[19] J. Baker-Jarvis, "Transmission/reflection and short-circuit line permittivity measurement methods," NIST, Gaithersburg, MD, USA, Tech. Note 1341, 1990, pp. 68–76.

FRANCK MOUKANDA MBANGO was born in Pointe-Noire, Republic of Congo, in 1973. He received an Engineering degree in microwave electronics from Mouloud Mammeri University, Algeria, in 2001, and the M.Sc. degree in microwave circuits from the National Polytechnic Institute (INP), in 2003, and the Ph.D. degree in microwave circuits the Joseph Fourier University at Grenoble, France, in 2008. From 2009 to 2014, he was involved in several telecommunication industrial projects as an Research and Development Engineer and a Research Assistant Consultant to ALTRAN Technologies for Vallourec, also as an Electromagnetic Compatibility (EMC) Engineer to Scientific and Technical Center for Building (CSTB). He is currently a CAMES Senior Lecturer and a Researcher with Marien Ngouabi University, Republic of Congo, and also a part-time Teacher with the Pan African University Institute for Basic Sciences Technology and Innovation (PAUISTI), Kenya. His research fields focus on high-frequency material measurement techniques, microwave device EM modeling for wireless applications, electromagnetic environment impact, electromagnetic modeling, and microwave design (antennas and circuits) systems.

JOSUÉ ERIC DELFORT M'PEMBA received the M.Sc. degree in electronics engineering systems from Marien Ngouabi University, Republic of Congo, in 2016, where he is currently pursuing the Ph.D. degree in microwave magnetic materials' characterization with the Laboratory of Electrical and Electronics Engineering. He has been holding the aptitude certificate for the Professorship of Technical Education with the Higher National Polytechnic College, Republic of Congo, since 1993. From 1996 to 2016, he has taught the analog and digital electronics at the sixth form named 'Lycée technique 1er Mai.' Since 2017, he has been a Delegate Inspector of technical education with the Electronics Department.

FABIEN NDAGIJIMANA received the Ph.D. degree in microwave and optoelectronics from the Institut National Polytechnique de Grenoble (INPG), France, in December 1990. In December 1990, he then joined the Faculty of Electrical Engineering ENSERG as an Associate Professor, where he teaches microwave techniques and electromagnetic modeling. Since September 1997, he joined the Université Grenoble Alpes, where he is currently a Full Professor with the Institut Universitaire de Technologie (IUT). He is currently a Professor with Université Grenoble Alpes, Grenoble, France. His research activity focuses on the characterization and electromagnetic modeling of microwave devices for wireless applications, signal integrity in high-speed applications, and test tools for electromagnetic compatibility standards.

BERNARD M'PASSI-MABIALA received the M.Sc. degree in physics from Martin Luther University, Germany, in 1982, and the Ph.D. degree in solid state physics from Strasbourg University, France, in 1996. As a Former Associate of the Abdus Salam International Centre of Theoretical Physics, Trieste, Italy, where he still involved in research activities, focus on electronic structure and magnetism of nanostructures, new material for energies, and renewable energies. Since 2010, he has been a CAMES Full Professor with the Faculty of Science and Technology (FST), Marien Ngouabi University (UMNG), where he lectures the theoretical physics, material science, and thermodynamics units. He has been the M.Sc. and Ph.D. Program Coordinator with FST, Material Sciences and Renewable Energies Department, since 2011. He has been the Vice President of the specialized technical committee in mathematics, physics and chemistry since 2014, and the PI and a Coordinator of the African Clean Energy Research Alliance (ACERA). Since 2018, he has also been the Manager Director of high education with the Ministry of High Education, Republic of Congo.